European Journal of Chemistry

View Journal Online
View Article Online

Synthesis and crystal structure of $[HexNH_3]_2[HC_2O_4]_2{\cdot}H_2O$: A novel hydrogen oxalate hydrate organic salt showing antimicrobial activity against *Streptomyces*

Mamadou Ba [1], Waly Diallo [1,*], Alhousseynou Sarr [2], Bocar Traoré [1], Daouda Ndoye [1], Nalla Mbaye [2], Mamadou Sidibé [1], Laurent Plasseraud [3] and Hélène Cattey [3,*]

[1] *Université Cheikh Anta Diop, Faculté des Sciences et Techniques, Département de Chimie, Laboratoire de Chimie Minérale et Analytique (LACHIMIA), Dakar, Sénégal*
[2] *Université Cheikh Anta Diop, Faculté des Sciences et Techniques, Département de Biologie Végétale, Laboratoire de Phytochimie et Protection Végétaux (LPPV), Dakar, Sénégal*
[3] *Université Bourgogne Europe, Institut de Chimie Moléculaire de l'Université de Bourgogne (ICMUB), UMR CNRS 6302, 9 Avenue Alain Savary, 21078 Dijon, France*

* *Corresponding author at: Université Cheikh Anta Diop, Faculté des Sciences et Techniques, Département de Chimie, Laboratoire de Chimie Minérale et Analytique (LACHIMIA), Dakar, Sénégal.*
e-mail: diallo_waly@yahoo.fr (W. Diallo), helene.cattey@ube.fr (H. Cattey).

RESEARCH ARTICLE

10.5155/eurjchem.16.3.251-258.2698

Received: 30 April 2025
Received in revised form: 04 July 2025
Accepted: 26 July 2025
Published online: 30 September 2025
Printed: 30 September 2025

KEYWORDS

Organic salt
Hydrogen bonds
Hydrogen oxalate
Antibacterial activity
X-ray crystal structure
Supramolecular assembly

ABSTRACT

The new monohydrated *n*-hexylammonium hydrogen oxalate salt $[HexNH_3]_2[HC_2O_4]_2{\cdot}H_2O$ (1) ($HexNH_3 = C_6H_{16}N^+$) has been prepared at room temperature, by mixing dehydrated oxalic acid with *n*-hexylamine. Salt 1 isolated as single-crystals, crystallizes in the orthorhombic system (space group $Pna2_1$) with cell constants of a = 14.1534(8) Å, b = 5.6656(3) Å, c = 26.8153(16) Å, V = 2150.3(2) Å^3 and Z = 4. Two *n*-hexylammonium cations, two hydrogen oxalate anions, and one water molecule compose the asymmetric unit. All components of salt 1 are linked through N-H···O and O-H···O hydrogen bonding interactions leading to an extended supramolecular self-assembly. Structural characterization of 1 was completed by infrared and UV-visible spectroscopy. Elemental analysis (C, H, and N) also corroborates the X-ray crystal structure. The antibacterial activity of salt 1 against a bacterial species of the genus *Streptomyces*, extracted from potatoes, was then investigated. The antibiotic susceptibility test revealed that the bacteria were highly sensitive to salt, from a concentration of 6 mg/mL, thus acting as an effective bactericide.

Cite this: *Eur. J. Chem.* **2025**, *16(3)*, 251-258 **Journal website**: www.eurjchem.com

1. Introduction

Crystal engineering, which consists of designing molecular solids through weak intermolecular interactions, is a research field in its own right, based on a strong interdisciplinary approach involving organic and coordination chemistry, supramolecular chemistry, crystallography, and solid-state chemistry [1]. The fields of application of crystal engineering are also numerous and varied, for example: gas sorption and storage, pharmaceutical polymorphs and co-crystals, solar energy conversion, and new prospects are emerging, such as mechanochemical synthesis and the response to antimicrobial resistance [2,3]. Dicarboxilic acid derivatives, in particular, oxalate and hydrogen oxalate, are reported to be suitable building blocks to design organic salts. They can be considered one of the simplest basic units capable of acting as both a donor and an acceptor. Combined with other synthons, such as amines, which are also well adapted as building blocks for crystal engineering [4,5], the possibilities for supramolecular constructions are endless. Numerous examples can be found in the literature. Several research groups, such as Ballabh *et al.*, Hayines and Pietersen, and Dzink *et al.* have described, for example, oxalate-based structures stabilized by ammonium cations [6-8]. Mac Donald *et* al., then Dziuk et al. have also published the architecture topology of secondary interactions in some oxalate compounds [9-11]. In coordination chemistry, the strong ability of the oxalate anion to coordinate with metal atoms has also encouraged many research groups to carry out work in this area [12]. In the biological field, oxalates are attracting growing interest due to their recognized antimicrobial activity [13-15]. This may be explained by the fact that in nature, oxalic acid and oxalates play a key role in the metabolism of plants, fungi, and bacteria [16].

https://dx.doi.org/10.5155/eurjchem.16.3.251-258.2698

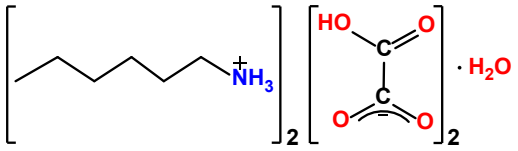

Figure 1. Molecular representation of $[C_6H_{16}N^+]_2[HC_2O_4^-]_2{\cdot}H_2O$ (1).

Recently, Braga *et al.* described the use of gallium oxalates as drug-drug salts showing antimicrobial performance against virulent bacterial strains [17]. In our laboratory, we have also been interested in these compounds for a long time and have published several crystallographic structures of organic salts and complexes derived from oxalates and hydrogen oxalates [18-20]. In this present article, we report the X-ray structure and spectroscopic characterization of the new hydrogen oxalate salt $[C_6H_{16}N^+]_2[HC_2O_4^-]_2{\cdot}H_2O$ (**1**) (Figure 1), prepared from oxalic acid and *n*-hexylamine. The objective of the present work falls within the framework of the fight against phytopathogenic bacteria that are responsible for bacterial diseases in plants. Therefore, the antibacterial activity of salt **1** against a bacterial species of the genus *Streptomyces*, extracted from potatoes, was studied.

2. Experimental

2.1. Material and measurements

Oxalic acid dihydrate ($H_2C_2O_4{\cdot}2H_2O$) was purchased from Merck while *n*-hexylamine ($HexNH_2$) was purchased from Aldrich Chemicals and used without further purification. The infrared spectrum was recorded using a PerkinElmer FT-IR spectrometer in the 4000-400 cm^{-1} region at Cheikh Anta Diop University in Dakar (Senegal). The UV-vis spectrum was recorded in H_2SO_4 (2 N) in the 200-1000 nm region with a speed of 600 nm/min and with strong smoothing using a Thermo Scientific Evolution 300 UV-VIS device controlled by Visionpro software. Elemental analysis was performed at the Plateforme d'Analyse Chimique et de Synthèse Moléculaire de l'Université de Bourgogne (PACSMUB) on a Fisons EA 1108 CHNS apparatus.

2.2. Synthesis and characterization of salt 1

The title salt was synthesized by mixing 0.252 g (2 mmol) of oxalate acid and 0.204 g (2 mmol) of *n*-hexylamine in 40 mL of water. The resulting colorless mixture was stirred at room temperature for 2 hours. After a few days of slow evaporation at 60 °C, 0.336 g of colorless single crystals were obtained with a yield of 74%. Analysis calculated for $C_{16}H_{36}N_2O_9$ (400.47): C, 47.99; H, 9.06; N, 7.00 Found: C, 47.89; H, 9.00; N, 6.83%. FT-IR (ATR, ν, cm^{-1}): 3341, 3042, 2955, 2928, 2857, 1923, 1722, 1687, 1602, 1517, 1473, 1398, 1340, 1217, 1098, 1040, 1017, 976, 968, 881,704, 481, 404. UV-visible data in H_2SO_4 (2 N): λ_{max} (nm): 295 ($n \rightarrow \pi^*$).

2.3. X-ray data collection and structure refinement

A suitable clear light colorless plate-shaped crystal with dimensions 0.25×0.10×0.08 mm^3 was mounted on a mylar loop oil. Data were collected using a Bruker Kappa Apex II CCD diffractometer operating at T = 110 K. Data were measured using f and w scans with Mo Kα radiation. The diffraction pattern was indexed and the total number of runs and images was based on the strategy calculation from the APEX3 program [21]. The maximum resolution achieved was Q = 27.602 ° (0.77). The unit cell was refined using SAINT V8.40B [22] on 9864 reflections, 16% of the observed reflections. Data reduction, scaling, and absorption corrections were performed using SAINT V8.40B. The final completeness is 99.90 % out to 27.602 in Q. SADABS-2016/2 [23] was used for absorption correction. wR_2(int) was 0.0532 before and 0.0467 after correction. The ratio of minimum to maximum transmission is 0.9447. The absorption coefficient m of this material is 0.100 mm^{-1} at this wavelength (λ = 0.71073Å) and the minimum and maximum transmissions are 0.704 and 0.746. The structure was solved and the space group $Pna2_1$ (# 33) was determined by the ShelXT 2018/2 structure solution program [24] using dual methods and refined by full matrix least squares minimization on F^2 using version 2018/3 of ShelXL 2018/3 [25]. All non-H atoms were refined anisotropically. Hydrogen atom positions were calculated geometrically and refined using the riding model. Programs used for the representation of the molecular and crystal structures: Olex2 [26], and Mercury [27]. Crystal data, data collection, and structure refinement details for compound **1** are summarized in Table 1. Bond lengths, bond angles, and torsion angles are listed in Tables 2-4, respectively.

2.4. Antibacterial method testing

The antimicrobial efficacy was evaluated as in previous work [28,29], according to current disk diffusion antibiotic susceptibility testing protocols [30]. The nonpathogenic Gram-positive culture used to test the antibacterial activity of salt **1** was *Streptomyce*. Antimicrobial activity was evaluated using the established antimicrobial disk zone of inhibition assay [31,32]. For the preparation of this culture medium, 23 g of powder of this nutrient agar (NA) were solubilized in 1 L of distilled water in a glass bottle. A clean magnetic bar is immersed in the bottle containing the mixture. This bottle is then placed on the stirrer so that the powder dissolves completely and a homogeneous solution is obtained. The medium was then autoclaved at 120 ° C with a pressure of 1.5 bar for sterilization for 45 minutes. After cooling for a few minutes, the supercooled medium is poured into Petri dishes, under the laminar flow hood to avoid any contamination during this operation. A suspension of the bacteria to be tested was made in a bottle containing physiological water. In each Petri dish containing the NA medium, 100 µL of this suspension was poured and spread using a glass spreader (modified Pasteur pipette) on the entire surface of the dish. The strain used is isolated from potato samples. This strain was stored in a freezer at 4 °C and sub-cultured once a week. When carrying out this test, the bacteria is transplanted onto the agar to rejuvenate it so that it is only 24 hours old.

Antimicrobial susceptibility testing was performed using modified microdilution of the following methods from the literature [33,34]. We used a bacterial strain of a species of the genus *Streptomyces* (Gram-positive bacteria) extracted from potatoes. The antibacterial activity of the salt was tested by the zone of inhibition test. For this purpose, disks of sterile Whatmann filter paper measuring 6 millimeters in diameter are impregnated with different concentrations (6, 10, and 20 mg/mL) of the salt previously dissolved in dimethylsulfoxide (DMSO). Using sterile forceps, the discs are placed on the surface of a medium seeded (spread) with a bacterial suspension.

Table 1. Crystal data and structure refinement for compound **1**.

Empirical formula	$C_{16}H_{36}N_2O_9$
Formula weight	400.47
Temperature (K)	110
Crystal system	orthorhombic
Space group	$Pna2_1$
a (Å)	14.1534(8)
b (Å)	5.6656(3)
c (Å)	26.8153(16)
α (°)	90
β (°)	90
γ (°)	90
Volume (Å^3)	2150.3(2)
Z	4
ρ_{calc} (g/cm^3)	1.237
μ/mm^{-1}	0.100
F(000)	872.0
Crystal size (mm^3)	0.25 × 0.1 × 0.08
Radiation	Mo Kα (λ = 0.71073)
2θ range for data collection (°)	5.756 to 55.204
Index ranges	$-18 \le h \le 18$, $-7 \le k \le 7$, $-34 \le l \le 34$
Reflections collected	60974
Independent reflections	4996 [R_{int} = 0.0312, R_{sigma} = 0.0148]
Data/restraints/parameters	4996/1/254
Goodness-of-fit on F^2	1.055
Final R indexes [I>=2σ (I)]	R_1 = 0.0269, wR_2 = 0.0674
Final R indexes [all data]	R_1 = 0.0309, wR_2 = 0.0697
Largest diff. peak/hole / e Å^{-3}	0.29/-0.14
Flack parameter	−0.3(9)

Table 2. Bond lengths for compound **1**.

Atom	Atom	Length (Å)	Atom	Atom	Length (Å)
O1	C13	1.317(2)	C1	C2	1.516(3)
O2	C14	1.242(2)	C2	C3	1.526(2)
O3	C14	1.259(2)	C3	C4	1.524(3)
O4	C13	1.204(2)	C4	C5	1.531(3)
C13	C14	1.553(2)	C5	C6	1.513(3)
O5	C15	1.312(2)	N2	C7	1.487(2)
O6	C15	1.204(2)	C7	C8	1.520(3)
O7	C16	1.258(2)	C8	C9	1.522(2)
O8	C16	1.242(2)	C9	C10	1.524(3)
C15	C16	1.553(2)	C10	C11	1.524(3)
N1	C1	1.491(2)	C11	C12	1.520(3)

Table 3. Bond angles for compound **1**.

Atom	Atom	Atom	Angle (°)	Atom	Atom	Atom	Angle (°)
O1	C13	C14	111.98(13)	O8	C16	C15	118.45(14)
O4	C13	O1	126.11(16)	N1	C1	C2	110.83(15)
O4	C13	C14	121.92(15)	C1	C2	C3	112.22(16)
O2	C14	O3	126.39(16)	C4	C3	C2	112.68(16)
O2	C14	C13	118.71(14)	C3	C4	C5	114.34(17)
O3	C14	C13	114.89(14)	C6	C5	C4	113.92(18)
O5	C15	C16	112.13(13)	N2	C7	C8	110.67(15)
O6	C15	O5	126.21(16)	C7	C8	C9	112.02(15)
O6	C15	C16	121.65(15)	C8	C9	C10	112.78(16)
O7	C16	C15	115.26(13)	C11	C10	C9	113.78(17)
O8	C16	O7	126.29(15)	C12	C11	C10	112.48(18)

Table 4. Torsion angles for compound **1**.

A	B	C	D	Angle (°)	A	B	C	D	Angle (°)
O1	C13	C14	O2	−7.7(2)	N1	C1	C2	C3	−173.86(15)
O1	C13	C14	O3	172.21(16)	C1	C2	C3	C4	−171.12(16)
O4	C13	C14	O2	172.16(18)	C2	C3	C4	C5	−175.59(17)
O4	C13	C14	O3	−8.0(2)	C3	C4	C5	C6	−63.8(2)
O5	C15	C16	O7	−169.48(16)	N2	C7	C8	C9	−170.70(14)
O5	C15	C16	O8	11.0(2)	C7	C8	C9	C10	−171.90(16)
O6	C15	C16	O7	10.6(3)	C8	C9	C10	C11	−173.67(16)
O6	C15	C16	O8	−168.88(18)	C9	C10	C11	C12	179.94(17)

The tests were repeated three times; disks impregnated with DMSO were also used (negative controls). All determinations are made in duplicate. After diffusion, the Petri dishes are then incubated in an oven for 18 to 24 hours at 37 °C. After incubation, the effect of the salt against the bacteria results in the appearance around the disc of a transparent circular zone reflecting the absence of bacterial growth, and then the zone of inhibition is measured.

3. Results and discussion

3.1. Synthesis

Compound **1** was isolated from a one-step process according to Equation 1. Aqueous solutions of oxalate acid ($H_2C_2O_4$) and *n*-hexylamine ($HexNH_2$) were mixed at room temperature and stirred for 2 hours.

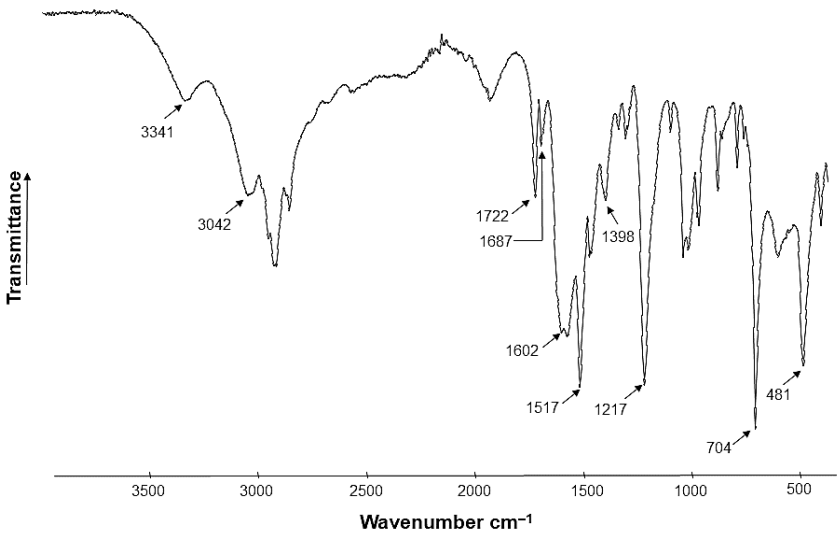

Figure 2. FT-IR spectrum (ATR mode) of salt **1**.

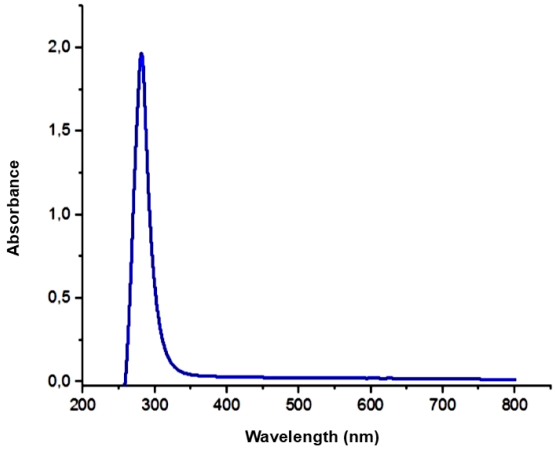

Figure 3. UV-vis absorption spectrum in H_2SO_4 solution (2 N) of salt **1**.

$$2C_2H_2O_4 + 2CH_3(CH_2)_5NH_2 + H_2O \xrightarrow[2h,\ 25°C]{} \underset{(1)}{[CH_3(CH_2)_5NH_3]_2[C_2HO_4]_2\cdot H_2O} \quad (1)$$

Single colorless crystals, suitable for XRD analysis, were collected from the supernatant solution and then characterized as $[HexNH_3]_2[HC_2O_4]_2\cdot H_2O$ (**1**). The yield of the reaction reported here is 74%, respectively.

3.2. FT-IR and UV-vis analyses

Crystals of salt **1** were first investigated by room temperature solid-state FT-IR spectroscopy in ATR mode. The spectrum recorded in the 4000-400 cm^{-1} range is shown in Figure 2. Characteristic absorption bands were assigned on the basis of previous data available in the literature [35-37]. The broad bands located at 3341 and 3042 cm^{-1} are assigned to ν(O–H) and ν(N-H) absorption bands, respectively. The bands at 2955, 2928 and 2857 cm^{-1} reflect ν(C–H) vibrations. The vibration bands at 1722 and 1687 cm^{-1} can be attributed to carbonyl absorptions. The $\nu_{as}(COO^-)$ and $\nu_s(COO^-)$ can be observed at 1602 and 1398 cm^{-1}, while the symmetric angular deformation of the $-NH_3^+$ group is revealed by a sharp band at 1517 cm^{-1}. The strong band, isolated at 1217 cm^{-1}, displays the elongation vibration of the C–C(O)–O group. Intense band at 704 cm^{-1} is attributed to O-C=O in plane bending vibrations and that at 481 cm^{-1} to O–C=O out of plane bending vibrations [38].

The UV-vis spectrum of the compound in H_2SO_4 solution (2 N) shows the presence of a single very strong electronic absorption band around 295 nm (Figure 3). This band is characteristic of the $n \rightarrow \pi^*$ transition of the COO^- carboxylate group of the oxalate anion [39].

3.3. Single-crystal X-ray diffraction

The asymmetric unit of the title salt is formed by two $HexNH_3^+$ cations, two $HC_2O_4^-$ hydrogen oxalate anions and one water molecule. The crystal structure of the salt **1** components is shown in Figure 4. The two $HC_2O_4^-$ are positioned parallel to each other, with their OH groups pointing in opposite directions. The orientation of $HexNH_3^+$ cations with respect to $HC_2O_4^-$ anions can be considered close to orthogonality. The dihedral angles between the planes involving N1-C1-C6 and O5-O8-C15-C16, and N2-C7-C12 and O1-O4-C13-C14 are 84° and 71°, respectively. The NH_3^+ groups of the two cations face each other. The values of the N-C bonds are identical of those reported by Thomas in $[Me_2NH_2]^+[HC_2O_4]^-$ [40].

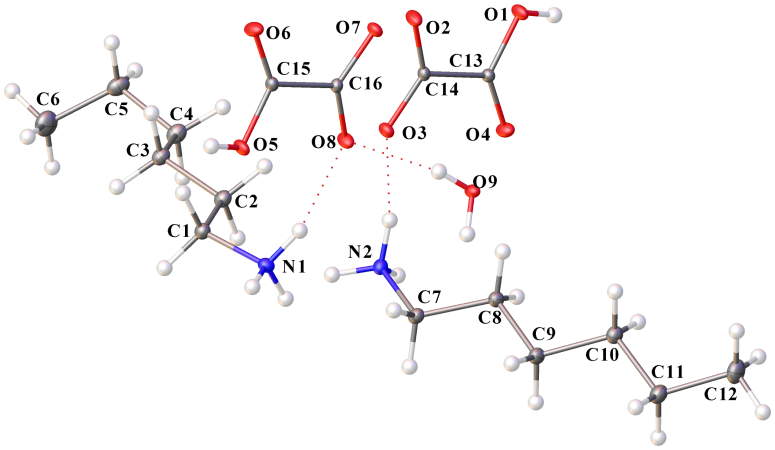

Figure 4. Crystal structure of salt **1** showing 30% probability ellipsoids for non-H atoms and the crystallographic numbering scheme (OLEX2 view) [atom color code: C, gray; H, white; N, blue; O, red].

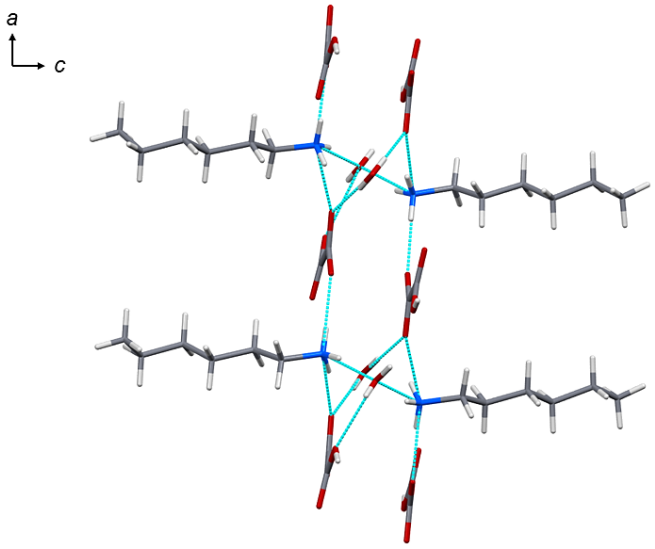

Figure 5. Molecular view along the *b*-axis of the hydrogen bonds (azure dash) involving $HC_2O_4^-$, H_2O and $HexNH_3^+$ (color code: blue-nitrogen, red-oxygen, grey-carbon, white-hydrogen).

A large number of structures involving alkylammonium cations are referenced in the CCDC structural database. To our knowledge, to date, 105 hits describe the presence of *n*-hexylammonium moieties. Several of these concerns the preparation of organic salts devoted to various purposes. For example, Rogers *et* al previously reported $[C_6H_{13}NH_3]^+[C_2H_3O_2]^-$ (CCDC code = QEYCII, 908843) with ionic liquid properties [41], Han *et al.* published $[C_6H_{13}NH_3]^+[C_4HO_4]^-\cdot{}^1/_2(H_2O)$ (CCDC code = UWASIX, 2087245) as 2D hydrogen-bonded molecular materials [42] and Dastidar *et al*. have deposited $[C_6H_{13}NH_3]_2^+[C_6H_6O_4]^{2-}$ (CCDC code = JEKJAL, 285967) with the aim of designing nanotubular architectures [43]. The isolation of salt **1** and the resolution of its X-ray structure provides a new example of an organic salt based on the *n*-hexylammonium cation, once again demonstrating the ability of alkylammoniums to promote hydrogen bonding interactions.

From a supramolecular point of view, interestingly, all components of salt **1** are interconnected, linked *via* N-H···O and O-H···O intermolecular hydrogen bonds leading to a complex three-dimensional network. Each NH_3^+ group of the *n*-hexylammonium cation interacts by hydrogen bonding with two oxygen atoms of two distinct hydrogen oxalate anion (N1-H ··O7 = 2.8103(18) Å, N1-H ··O8 = 2.8327(19) Å, N2-H ··O2 = 2.837(2) Å, N2-H ··O3 = 2.8064(19) Å) and with the water molecule that co-crystallized within salt **1** (N1-H ··O9 = 2.7787(19) Å, N2-H ··O9 = 2.785(2) Å) (Figure 5). Thus, the distances of the N-H ··O hydrogen bonds are shorter in the case of water molecules than in the case of hydrogen oxalates. In both cases, these values are comparable to those described previously in the literature [18-20]. In addition, the two hydrogen oxalates present in salt **1** are also linked together. They form *via* O–H···O interactions (O1-H···O3 = 2.5857(16) Å, O5-H···O7 = 2.5884(16) Å), two parallel offset strands propagating along the *b*-axis. The result is an organization that can be compared to channel formation, joined along the *a* axis by water molecules in hydrogen bonding interaction and that bridge hydrogen oxalates of two distinct strands (Figure 6). (O9-H···O8 = 2.7334(17) Å, O9-H···O2 = 2.7307(17) Å). The carbon chains of $HexNH_3^+$ cations are also aligned and positioned almost perpendicular to hydrogen oxalate-based channels. A representation of the final supramolecular architecture of salt **1** is shown in Figure 7.

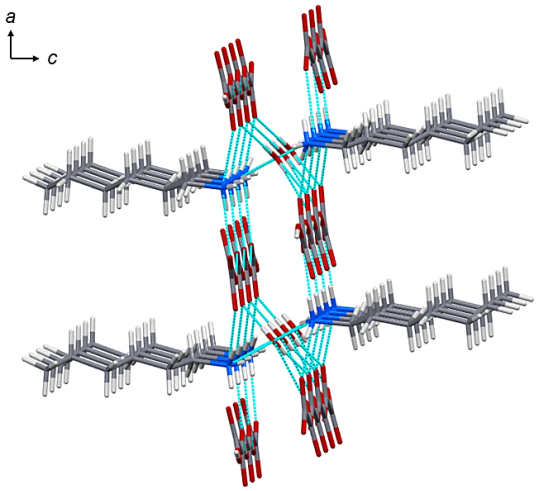

Figure 6. Focus on the channel-shaped structure. Hydrogen bonds are represented by azure dashes (color code: blue–nitrogen, red-oxygen, grey-carbon, white-hydrogen).

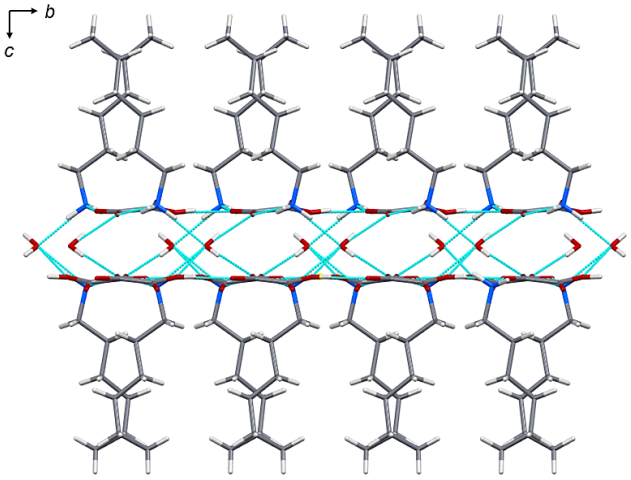

Figure 7. Molecular view along the *a*-axis of the resulting supramolecular network. Hydrogen bonds are highlighted by azure dashes (color code: blue-nitrogen, red-oxygen, grey-carbon, and white-hydrogen).

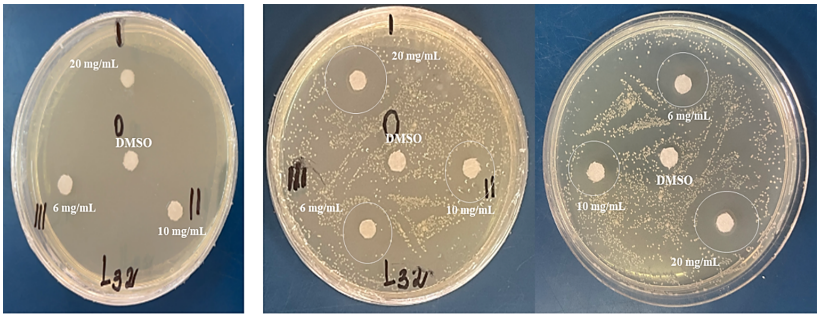

Figure 8. Inhibition zone test of the title compound in a Gram-positive bacterial species (*Streptomyces*) extracted from a potato in the St-Louis/Senegal area (left: before incubation, right: after 24 hours incubation).

3.4. Antibacterial activity study

The antibacterial activity of salt **1** against *Streptomyces* was tested with three increasing concentrations: 6, 10 and 20 mg/mL. As shown in the pictures in Figure 8, an inhibition zone is observed from the lowest concentration value. Salt **1** clearly exhibits very significant antibacterial activity against *Streptomyces*. The 20 mg/mL concentration again increased the impact on bacterial growth, leading to a higher zone of inhibition (Figure 9). According to Cho *et al*., we can conclude that at concentrations of 6 and 10 mg/mL, *Streptomyces* are very sensitive to salt **1** and become extremely sensitive with a concentration of 20 mg/mL [44]. As far as the bactericidal action of salt **1** is concerned, we can at this stage try to explain it by: (i) the presence of several donor atoms (oxygen and nitrogen) in the molecule, which gives it good stability, and (ii) the ability of the oxalate anion to be an easy and versatile ligand that can lead to different coordination modes (monodentate, bidentate or chelating).

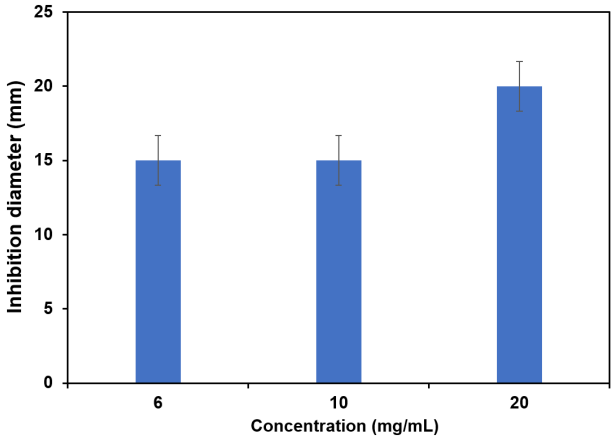

Figure 9. Antibacterial activity of $[HexNH_3]_2[C_2O_4]_2{\cdot}H_2O$ (**1**) against *streptomyce* (Gram-positive bacteria).

4. Conclusions

With antimicrobial resistance increasing, the development of new, effective organic and inorganic compounds is a growing challenge that needs to be addressed urgently. *Streptomyces* bacterium is one of the main bacterial species that cause serious problems for Senegalese agriculture, as it attacks potato and mango leaves, severely reducing harvests. In this study, we describe the synthesis and structural characterization of a new organic salt, identified as $[HexNH_3]_2[HC_2O_4]_2{\cdot}H_2O$ (**1**), showing in the solid state a highly developed hydrogen bonding network. The antibacterial activity of this compound was also tested, demonstrating its inhibitory action against *Streptomyces* bacteria. In the future, we will continue this work to better understand the possible correlation that may exist between the molecular and supramolecular structures of the organic salt and their impact on antimicrobial activity.

Acknowledgements

We thank the general and financial supports from the University Cheikh Anta Diop-Dakar (Senegal), the University of Bourgogne Europe (France), and the Centre National de la Recherche Scientifique (CNRS-France).

Supporting information

CCDC-2447471 contains the supplementary crystallographic data for this article. These data can be obtained free of charge from the Cambridge Crystallographic Data Centre via https://www.ccdc.cam.ac.uk/data-request/cif or from the Cambridge Crystallographic Data Centre, 12 Union Road, Cambridge CB2 1EZ, UK; fax: +44(0)1223-336033; or e-mail: deposit@ccdc.cam.ac.uk.

Disclosure statement

Conflict of interest: The author declares that they have no conflict of interest.
Ethical approval: All ethical guidelines have been followed.
Sample availability: Samples of the compound are available from the author.

Funding

Research was carried out at Cheikh Anta Diop University in Dakar, Senegal, and is funded by the Senegalese Government.

CRediT authorship contribution statement

Conceptualization: Waly Diallo; Methodology: Waly Diallo, Laurent Plasseraud, Nalla Mbaye, Mamadou Sidibé, Hélène Cattey ; Software: Hélène Cattey; Validation: Waly Diallo, Laurent Plasseraud, Nalla Mbaye; Formal Analysis: Waly Diallo, Laurent Plasseraud, Hélène Cattey; Investigation: Waly Diallo, Laurent Plasseraud, Hélène Cattey; Resources: Bocar Traoré, Daouda Ndoye, Nalla Mbaye, Mamadou Sidibé; Data Curation: Mamadou Ba, Waly Diallo, Alhousseynou Sarr; Writing - Original Drafts: Waly Diallo; Writing - Review and Editing: Laurent Plasseraud, Hélène Cattey, Waly Diallo; Visualization: Laurent Plasseraud, Waly Diallo; Supervision: Waly Diallo, Laurent Plasseraud; Project Administration: Waly Diallo, Laurent Plasseraud.

ORCID and Email

Mamadou Ba
mamadou146.ba@ucad.edu.sn
https://orcid.org/0009-0005-4931-5585
Waly Diallo
waly.diallo@ucad.edu.sn
https://orcid.org/0009-0001-9625-0973
Alhousseynou Sarr
alhouseynou97@gmail.com
https://orcid.org/0009-0007-6426-205X
Bocar Traoré
bocar.traore@ucad.edu.sn
https://orcid.org/0009-0002-6385-4639
Daouda Ndoye
ndoyedeve@yahoo.fr
https://orcid.org/0009-0005-7612-8136
Nalla Mbaye
nalla.mbaye@ucad.edu.sn
https://orcid.org/0009-0001-5423-8239
Mamadou Sidibé
mamadou4.sidibe@ucad.edu.sn
https://orcid.org/0000-0002-5499-1087
Laurent Plasseraud
laurent.plasseraud@u-bourgogne.fr
https://orcid.org/0000-0002-7870-1881
Hélène Cattey
helene.cattey@u-bourgogne.fr
https://orcid.org/0000-0002-4416-7510

References

[1]. Braga, D. Crystal engineering, Where from? Where to?. *Chem. Commun.* **2003**, 2751.
[2]. Nangia, A. K.; Desiraju, G. R. Crystal Engineering: An Outlook for the Future. *Angew. Chem. Int. Ed.* **2019**, *58* (13), 4100–4107.
[3]. Braga, D. Crystal engineering: from promise to delivery. *Chem. Commun.* **2023**, *59* (95), 14052–14062.
[4]. Mo, L.; Jin, S.; Zhang, W.; Guo, J.; Liu, H.; Wang, D. The crystal structures of ten supramolecular adducts of benzylamine and organic acids. *J. Mol. Struc.* **2020**, *1205*, 127538.
[5]. Yang, X.; Zhu, Y.; Chen, X.; Gao, X.; Jin, S.; Liu, B.; He, L.; Chen, B.; Wang, D. Molecular structures of ten ionic hydrogen bond-mediated anhydrous tert-butylammonium salts from different carboxylic acids. *J. Mol. Struc.* **2022**, *1251*, 131917.
[6]. Ballabh, A.; Trivedi, D. R.; Dastidar, P.; Suresh, E. Hydrogen bonded supramolecular network in organic salts: crystal structures of acid–

base salts of dicarboxylic acids and amines. *CrystEngComm.* **2002**, *4* (24), 135–142.
[7]. Haynes, D. A.; Pietersen, L. K. Hydrogen bonding networks in ammonium carboxylate salts: the crystal structures of phenylethylammonium fumarate-fumaric acid, phenylethylammonium succinate-succinic acid and anilinium fumarate-fumaric acid. *CrystEngComm.* **2008**, *10* (5), 518.
[8]. Dziuk, B.; Ejsmont, K.; Zaleski, J. Crystalline structures of salts of oxalic acid and aliphatic amines. *Chemik*, **2014**, *68*, 391–395. https://www.europub.co.uk/articles/crystalline-structures-of-salts-of-oxalic-acid-and-aliphatic-amines-A-110304
[9]. MacDonald, J. C.; Dorrestein, P. C.; Pilley, M. M. Design of Supramolecular Layers via Self-Assembly of Imidazole and Carboxylic Acids. *Crystal Growth & Design* **2000**, *1* (1), 29–38.
[10]. Dziuk, B.; Zarychta, B.; Ejsmont, K. Allylammonium hydrogen oxalate hemihydrate. *Acta. Crystallogr. E. Struct. Rep. Online* **2014**, *70* (8), o852–o852.
[11]. Dziuk, B.; Zarychta, B.; Ejsmont, K. Crystal structure of allylammonium hydrogen succinate at 100 K. *Acta. Crystallogr. E. Struct. Rep. Online* **2014**, *70* (9), o917–o918.
[12]. Haiduc, I. Inverse coordination metal complexes with oxalate and sulfur, selenium and nitrogen analogues as coordination centers. Topology and systematization. *J. Coord. Chem.* **2020**, *73* (11), 1619–1700.
[13]. Jayashri, T.; Krishnan, G.; Viji, K. Spectral, Thermal and Antimicrobial Studies of Gamma Irradiated Potassium Diaquabis (Oxalato) Cobaltate (II). *Orient. J. Chem.* **2017**, *33* (1), 371–377.
[14]. Ameen, M.; Gilini, S. R.; Naseer, A.; Shoukat, I.; Ali, S. D.; Sadiqa, A. Synthesis and Antibacterial Activities of Mixed Ligands Complexes of Cu(II) and Zn(II) Containing Tridentate Azo Anils Ligands and Bidentate Oxalate Ion. *Asian. J. Chem.* **2015**, *27* (11), 3988–3992.
[15]. Darling, D. A.; Joema, S. E. Antibacterial activity, optical, mechanical, thermal, and dielectric properties of L-phenylalanine fumaric acid single crystals for biomedical, optoelectronic, and photonic applications. *J. Mater. Sci: Mater. Electron* **2020**, *31* (24), 22427–22441.
[16]. Grąz, M. Role of oxalic acid in fungal and bacterial metabolism and its biotechnological potential. *World. J. Microbiol. Biotechnol.* **2024**, *40* (6), 178 https://doi.org/10.1007/s11274-024-03973-5.
[17]. Guerrini, M.; d'Agostino, S.; Grepioni, F.; Braga, D.; Lekhan, A.; Turner, R. J. Antimicrobial activity of supramolecular salts of gallium(III) and proflavine and the intriguing case of a trioxalate complex. *Sci. Rep.* **2022**, *12* (1), 3673 https://doi.org/10.1038/s41598-022-07813-0.
[18]. Diallo, W.; Gueye, N.; Crochet, A.; Plasseraud, L.; Cattey, H. Crystal structure of dimethylammonium hydrogen oxalate hemi(oxalic acid). *Acta. Crystallogr. E. Cryst. Commun.* **2015**, *71* (5), 473–475.
[19]. Diop, M. B.; Diop, L.; Plasseraud, L.; Cattey, H. Crystal structure of 2-methyl-1*H*-imidazol-3-ium hydrogen oxalate dihydrate. *Acta. Crystallogr. E. Cryst. Commun.* **2016**, *72* (8), 1113–1115.
[20]. Toure, A.; Diop, C. A.; Diop, L.; Plasseraud, L.; Cattey, H. Ethylammonium hydrogen oxalate–oxalic acid (2/1). *IUCrData* **2019**, *4* (5), x190635 https://doi.org/10.1107/S2414314619006357.
[21]. Bruker (2020). APEX3. Bruker AXS Inc., Madison, Wisconsin, USA.
[22]. Bruker (2016) SAINT V8.40B - Software for the Integration of CCD Detector System Bruker Analytical X-ray Systems, Bruker AXS Inc.: Madison, Wisconsin, USA.
[23]. Bruker (2016) SADABS-Bruker Nonius Area Detector Scaling and Absorption Correction -V2016/2; Bruker AXS Inc.: Madison, WI, USA.
[24]. Sheldrick, G. M. *SHELXT*– Integrated space-group and crystal-structure determination. *Acta. Crystallogr. A. Found. Adv.* **2015**, *71* (1), 3–8.
[25]. Sheldrick, G. M. Crystal Structure Refinement with SHELXL. *Acta Crystallogr. C Struct. Chem.* **2015**, *71* (Pt 1), 3–8.
[26]. Dolomanov, O. V.; Bourhis, L. J.; Gildea, R. J.; Howard, J. A.; Puschmann, H. *OLEX2*: a complete structure solution, refinement and analysis program. *J. Appl. Crystallogr.* **2009**, *42* (2), 339–341.
[27]. Macrae, C. F.; Bruno, I. J.; Chisholm, J. A.; Edgington, P. R.; McCabe, P.; Pidcock, E.; Rodriguez-Monge, L.; Taylor, R.; van de Streek, J.; Wood, P. A. *Mercury CSD 2.0*– new features for the visualization and investigation of crystal structures. *J. Appl. Crystallogr.* **2008**, *41* (2), 466–470.
[28]. Fiore, C.; Shemchuk, O.; Grepioni, F.; Turner, R. J.; Braga, D. Proflavine and zinc chloride "team chemistry": combining antibacterial agents *via* solid-state interaction. *CrystEngComm.* **2021**, *23* (25), 4494–4499.
[29]. Shemchuk, O.; Braga, D.; Grepioni, F.; Turner, R. J. Co-crystallization of antibacterials with inorganic salts: paving the way to activity enhancement. *RSC. Adv.* **2020**, *10* (4), 2146–2149.
[30]. Balouiri, M.; Sadiki, M.; Ibnsouda, S. K. Methods for in vitro evaluating antimicrobial activity: A review. *Journal of Pharmaceutical Analysis* **2016**, *6* (2), 71–79.
[31]. Performance Standards for Antimicrobial Disk Susceptibility Tests, Approved Standard. CLSI Document M02-A11 7th Edition; 2012.
[32]. Hudzicki, J. Kirby-Bauer Disk Diffusion Susceptibility Test Protocol. 2009. https://asm.org/getattachment/2594ce26-bd44-47f6-8287-0657aa9185ad/kirby-bauer-disk-diffusion-susceptibility-test-protocol-pdf.pdf
[33]. Fatima, H.; Khan, K.; Zia, M.; Ur-Rehman, T.; Mirza, B.; Haq, I. Extraction optimization of medicinally important metabolites from Datura innoxia Mill.: an in vitro biological and phytochemical investigation. *BMC. Complement. Altern. Med.* **2015**, *15* (1), https://doi.org/10.1186/s12906-015-0891-1.
[34]. Sharma, A.; Chandraker, S.; Patel, V.; Ramteke, P. Antibacterial activity of medicinal plants against pathogens causing complicated urinary tract infections. *Indian. J. Pharm. Sci.* **2009**, *71* (2), 136.
[35]. Nakamoto, K. Infrared and Raman Spectra of Inorganic and Coordination Compounds. John Wiley & Sons, 2008, https://doi.org/10.1002/9780470405888.
[36]. Mangaiyarkarasi, K.; Ravichandran, A.; Anitha, K.; Manivel, A. Synthesis, growth and characterization of L-Phenylalaninium methanesulfonate nonlinear optical single crystal. *J. Mol. Struc.* **2018**, *1155*, 758–764.
[37]. Hug, S. J.; Bahnemann, D. Infrared spectra of oxalate, malonate and succinate adsorbed on the aqueous surface of rutile, anatase and lepidocrocite measured with in situ ATR-FTIR. *Journal of Electron Spectroscopy and Related Phenomena* **2006**, *150* (2-3), 208–219.
[38]. Hamdouni, M.; Agengui, L.; Walha, S.; Kabadou, A.; Ben Salah, A. Synthesis and Crystal Structure of a New Mixed Alkali Oxalate A1−x (NH4) x (H2C2O4)(HC2O4)(H2O)2 with A = K, Rb. *J. Chem. Crystallogr.* **2011**, *41* (11), 1742–1750.
[39]. Lund Myhre, C. E.; Nielsen, C. J. Optical properties in the UV and visible spectral region of organic acids relevant to tropospheric aerosols. *Atmos. Chem. Phys.* **2004**, *4* (7), 1759–1769.
[40]. Thomas, J. O. Hydrogen Bond Studies. CXXII. A Neutron Diffraction and X–N Deformation-Electron-Density Study of Dimethylammonium Hydrogen Oxalate, (CH3)2NH2HC2O4, at 298 K. *Acta Crystallogr. B* **1977**, *33* (9), 2867–2876.
[41]. McCrary, P. D.; Beasley, P. A.; Gurau, G.; Narita, A.; Barber, P. S.; Cojocaru, O. A.; Rogers, R. D. Drug specific, tuning of an ionic liquid's hydrophilic–lipophilic balance to improve water solubility of poorly soluble active pharmaceutical ingredients. *New. J. Chem.* **2013**, *37* (7), 2196.
[42]. Liu, L.; Miao, L.; Han, X.; Zhang, W. 2D Hydrogen-Bonded Molecular Crystals Showing Terminal-Group-Triggered Phase Transitions and Dielectric Responses. *Crystal Growth & Design* **2021**, *21* (9), 5342–5348.
[43]. Ballabh, A.; Trivedi, D. R.; Dastidar, P. From Nonfunctional Lamellae to Functional Nanotubes. *Org. Lett.* **2006**, *8* (7), 1271–1274.
[44]. Cho, Y. M.; Kwon, S.; Pak, Y. K.; Seol, H. W.; Choi, Y. M.; Park, D. J.; Park, K. S.; Lee, H. K. Dynamic changes in mitochondrial biogenesis and antioxidant enzymes during the spontaneous differentiation of human embryonic stem cells. *Biochemical and Biophysical Research Communications* **2006**, *348* (4), 1472–1478.